

Strain analysis of Jonk River Conglomerate, Sonakhan Greenstone Belt, Distt – Balodabazar, Chhattisgarh

Ketan Chourasia¹, Dr. P. Diwan²

Author's Affiliations:

¹Department of Geology, Vishwavidyalaya Engineering College, Lakhanpur, Ambikapur, Chhattisgarh 497116, India

²Department of Applied Geology, National Institute of Technology, Raipur, Chhattisgarh 492010, India.

***Corresponding Author:** Ketan Chourasia, Department of Geology, Vishwavidyalaya Engineering College, Lakhanpur, Ambikapur, Chhattisgarh 497116, India

E-mail: ketangrd21@gmail.com

(Received on 23.06.2018, Accepted on 11.07.2018)

Abstract

The Jonk River Conglomerate refers to the structure where the outcrop pattern in the area include pebbles lineation developed due to parallel arrangement of stretched pebbles, fold axis and intersection lineation developed due intersection of S_0 and S_1 . Two deformations event have affects the Sonakhan Greenstone Rocks. The second phase of deformation is represented by broad and open flexures (F_2) having NE-SW trending axial planes. Strain analysis on the five arbitrarily chosen structural domain (D1 – D5) from the area was performed in YZ section with Elliott polar plot, Fry methods and whole rock strain analysis was performed by Flinn methods and logarithmic Flinn methods. The strain data show that conglomerate from the area exhibit Flattening to plain strain ellipsoid. The strain results of Flinn methods and Logarithmic Flinn methods show consistent volume loss and shortening from D1 to D5.

Keywords: Strain Analysis, Deformations, Elliott polar plot, Fry Methods, Flinn Methods, Logarithmic Flinn Methods, Volume Loss and Shortening.

1. Introduction

Geological strain analysis is common procedure for quantitative estimation of amount of deformation in the rocks. Conglomerates that contain stretched pebbles can be used for strain analysis and the determination of the finite strain on a regional scale (Ramsay, 1967; Hossack, 1968; Dunnet, 1969; Elliot, 1970; Lisle, 1979; Babaie, 1986; Treagus and Treagus, 2002; Mulchrone et al., 2005). Finite Strain determination can be carried out by noting principal strain axis for strain marker such as conglomerate pebbles. Many workers have developed different techniques to quantify strain in conglomerate. The first 3D strain analysis was carried out by D Flinn in 1956, popularly known as Flinn's analysis. In early studies by Hossack (1968), Burns and Spary (1969) and Gay (1969), it was largely assumed that the ellipsoid pebble of conglomerate shows relict feature of deformation stages. Ramsay (1967) and Ramsay and Hubber (1983) each provide comprehensive review of methods in the

analysis of strain in conglomerates. While for the two-dimensional strain plot, a graphical technique was introduced by Elliot, 1970, known as polar Elliott plots, which are types of hyperboloidal projections. Hyperboloidal projections are analogous to spherical projections, such as the stereographic and equal-area projections that are used to create stereonet and Schmidt nets respectively, familiar to structural geologists. The polar plot is not a unique graphical representation of the shape-orientation relationship. For example, the R/ϕ plot is an option. The polar plot has an advantage in that it has no mathematical singular point. That is, every point on the plot represents a unique shape and an orientation, and vice versa (Fig 1). Accordingly, the plot is convenient for mathematical analyses. In contrast, the R/ϕ plot has singularity in that the circular shapes are represented by infinitely many points on the line $R = 1$ that is parallel to the ϕ axis.

In order to find the volume loss and shortening in spatially distributed area, the logarithmic Flinn plot method was used. The Logarithmic Flinn diagram is a logarithmic version of Flinn diagram introduced by Ramsay (1967). Ramsay introduced this modification of Flinn diagram that can be used to keep track of changes in volume that might accompany distortion. The results were discussed in table 4 & 5.

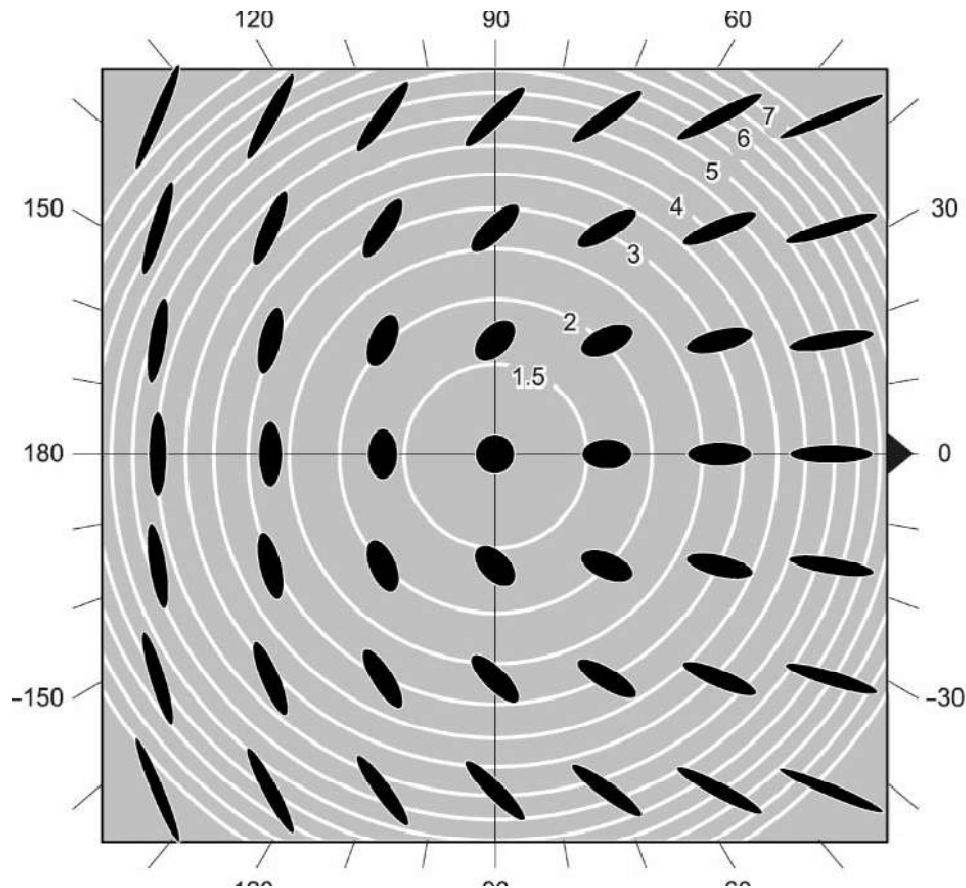


Figure 1: Ellipses represented by grid points on the polar plot. Circles indicate equal-aspect-ratio lines on which numbers are placed to indicate the ratio. The center of this diagram represents a circle. The ratio is plotted by a logarithmic scale.

For the computation of Elliott polar plot and Fry methods, computer-based programme is used called *EllipseFit 3.4.0* software (Vollmer, 2011) while for the computation of Flinn's diagram *Flinn Plot* (Roday, 2003) is used. *EllipseFit* is suitable for determining two- and three-dimensional strain using various objects including centre points (Fry analysis), lines, ellipses, and polygons. *EllipseFit* includes procedures for complete fabric and strain analyses, including image processing, digitizing, calculation of two-dimensional sectional ellipses, and combination of sections to obtain three-dimensional ellipsoids (Vollmer, 2011). For Flinn diagram, the Flinn plot software is written by P. P. Roday, 2003, for Windows 32-Bit Platform Software for plots to display the finite strain data. Based on the strain results provided in table 1, 2, 3, 4 & 5, dilation within the five structural domain (D1 – D5) was calculated using Strain Det Progs (a software by Prakash Rody) that is based on the Log Flinn diagram suggested by Ramsay, 1967. The software provided negative values of dilation which means loss in volume.

2. Geological Setting

The Sonakhan greenstone belt of Central Indian Cratonic (CIC)/Bastar block of central India is a classic example late Archean – Paleoproterozoic greenstone belt in India. It covers an area of about 1200 sq. km. The Sonakhan granite green stone belt trends NNW-SSE direction for about 40km from Sonakhan in the north to Remra (21°17"N: 82°46"E). The Sonakhan group of Paleoproterozoic divided into lower Baghmara formation, middle formation as Arjuni and upper Bilari formation. The lower predominantly consists of volcanic suites, mainly meta-ultramafites, schistose and massive metabasalt, meta-gabbro, pyroclastics of intermediates to basics composition, ignimbrite, rhyolites, acidic tuff, pebbly tremolite-actinolite schist, carbonaceous argillite and ferruginous sulphide-bearing chert (Mondal *et. al*, 2009). The upper formation Arjuni unconformably overlies the Baghmara formation by a thick sedimentary pile and starts with Jonk river conglomerate. The Jonk river conglomerate marks the unconformity between the Baghmara formation and Arjuni formation, which is polymictic in nature and demonstrate bimodality in matrix composition. The matrix is mainly meta – arkosic and chlorite /biotite rich greywacke but at some place near to Rajadevri and upto north Arjuni, it is totally replacing by volcanic materials. The Jonk conglomerate is sandwiched between Baghmara and Arjuni formation and constricted to Jonk river only (Das, *et. al*. 1990). The conglomerate horizon is marked by ill-sorted pebble, cobbles and boulders with preserved striations marks. The pebbles of granite, gneiss, acidic volcanic rocks, porphyries, amphibolite, metabasalts, quartzites, quartz veins, BIF, jasper, phyllites and schists. Since the strain analysis of conglomerates can give the true results if the clast matrix ratio is assumed to be low as 90:10. Here the clast versus matrix ratio varies with average from 90:10 to 10:90. Bilari Group essentially comprises basic and acid intrusive and extrusive, (Figure 2.) (Das, *et. al*. 1990). All three-formation rest on a gneissic basement, the Baya gneissic complex (Chawade, 2010).

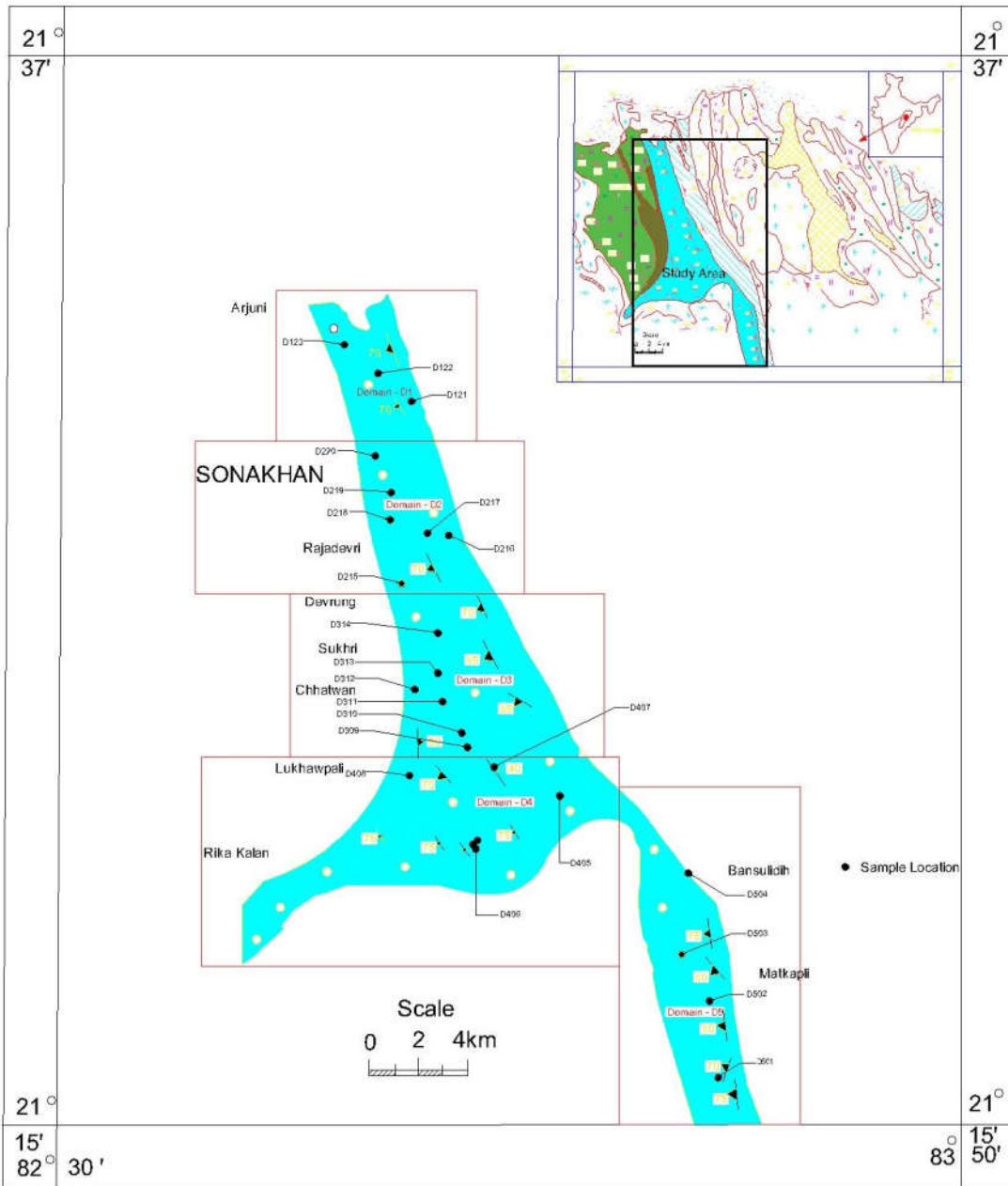


Figure 2: Conglomerate horizon map showing sample location.

3. Structural Setup

The Sonakhan Greenstone Belt represents a broad synformal basin with moderate plunge to the North – Northwest and closure to the south near Baya (*Das et al., 1990*). Two phases of deformation have been observed in the Sonakhan Greenstone Belt. The first phase is represented by first generation of fold (F_1) best developed in BIF and chert bands of Arjuni Formation. These folds are open to tight and steeply inclined to upright with their axial surface running parallel to the regional trend that is NNW – SSE. They show moderate to steep plunge towards NNW. The repetition of various lithounits of SGB is the result of F_1 folds.

The second phase of deformation is represented by broad and open flexures (F_2) having NE-SW trending axial plane. They have developed variable plunge in the F_1 axes due to superimposed folding.

The planar structures in the area include stratification (S_0) in BIF and chert bands schistosity (S_1) developed in the metabasalts and schists due to parallel arrangement of chlorite and actinolite grains. Generally, a westerly dip ranging from 65° to 82° was observed along the foliation planes and flow layers of metabasalts. The planar structures include those developed due to flattening and preferred orientation of pillows in metabasalts and clasts in Jonk Conglomerate.

The linear structure in the area include pebble lineation in Jonk conglomerate developed due to parallel arrangement stretched pebbles, fold axis and intersection lineation developed due to intersection of S_0 and S_1 .

The major trends of lineaments and faults in the study area is parallel to the regional trend of the sonakhan greenstone belt i.e. NNW-SSE. Presence of minor faults in the region is often punctuated by the field evidences like silicification and mineralization, presences of mylonite slickensides.

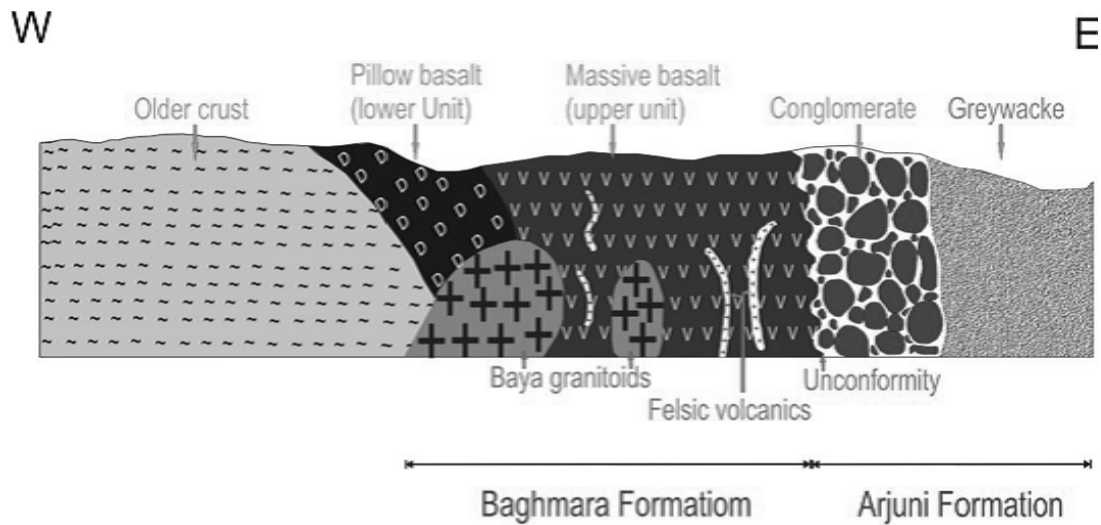


Figure 3: Schematic E-W cross section showing relationships among different litho-units of the Sonakhan Greenstone belt. (From Mondal and Raza, 2009)

4. Methodology

The Jonk River Metaconglomerate basal section of Arjuni Formation marks the unconformity to Baghmara formation. Whole length of 24 km of conglomerate horizon is demarked arbitrarily with five structural domains named as D1 to D5 as shown in map (Fig.2). In this study, these metaconglomerate pebbles are used to determine finite strain (R_s) and volume loss in the rock while deformation. The lineation of the sample from each domain represents the longest axis (X) of the strain ellipsoid on the XZ plane. The shortest axis (Y) is normal to the X on the XZ plane. The YZ plane contains the intermediate axis (y) as well as the shortest axis (Z) of the strain ellipse. Length-to-width ratios of pebbles were determined from measurements made on YZ plane which is nearly horizontal, parallel and perpendicular to the schistosity plane. For the Elliott polar plot and Fry methods YZ plane photographs are used.

4.1 Flinn Method

However, for the Flinn method, measurement taken from the outcrop, by noting the strain principal planes and converting the data from two dimensions into three-dimensional data (Ramsay, 1967; Dunnet, 1969). Hence, the whole – rock strain (Bulk Strain) from clast are calculated. Flinn graph plots the value of R_{yz} as abscissa and R_{xy} as the ordinate (Flinn, 1962). The origin of the graph is not the point

(0,0) but the point (1,1) because R values of less than unity cannot, by definition, exist. Flinn suggest the parameter k to describe the general position of the ellipsoid plot. The k - value is defined as

$$k = \frac{R_{xy} - 1}{R_{yz} - 1} \dots \dots \dots (I)$$

$$R_{xy} = \frac{R_{xz}}{R_{yz}} \dots \dots \dots (II)$$

Where R_{xy} is the finite strain on the XY plane (foliation), R_{yz} is the finite strain on the YZ plane, and R_{xz} is the finite strain on the XZ plane. Figure 4(a-e) is Flinn diagram of each arbitrarily chosen structural domain from D1 to D5 of various localities. It is worth to notice that k values progressively approaching lower value from Arjuni (North) to Matkapali (South).

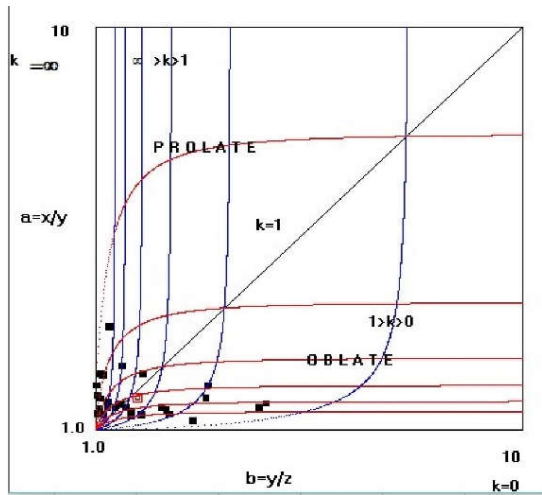


Figure 4a: Flinn diagram for location D1-23

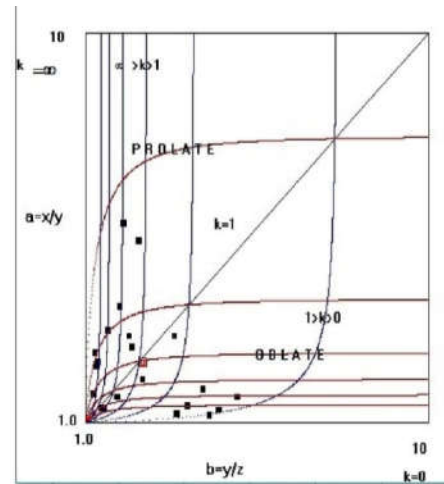


Figure 4b: Flinn diagram for location D2-19

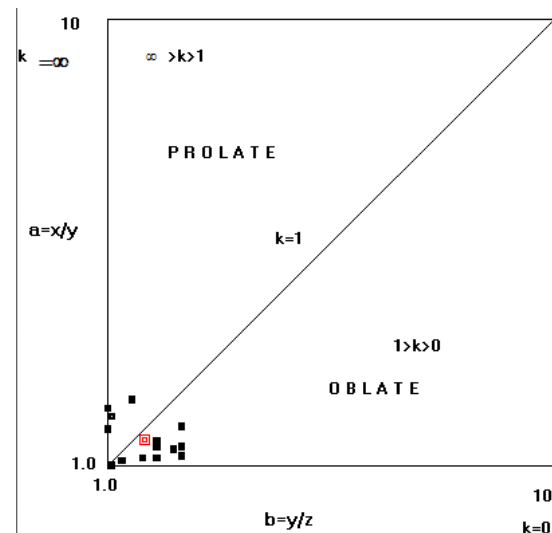


Figure 4c: Flinn diagram for location D3-11

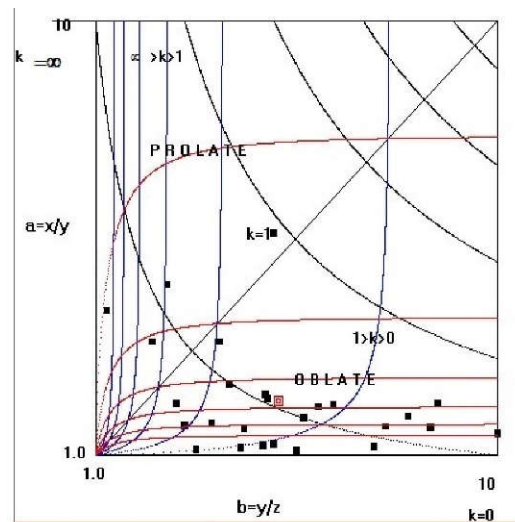


Figure 4d: Flinn diagram for location D4-07

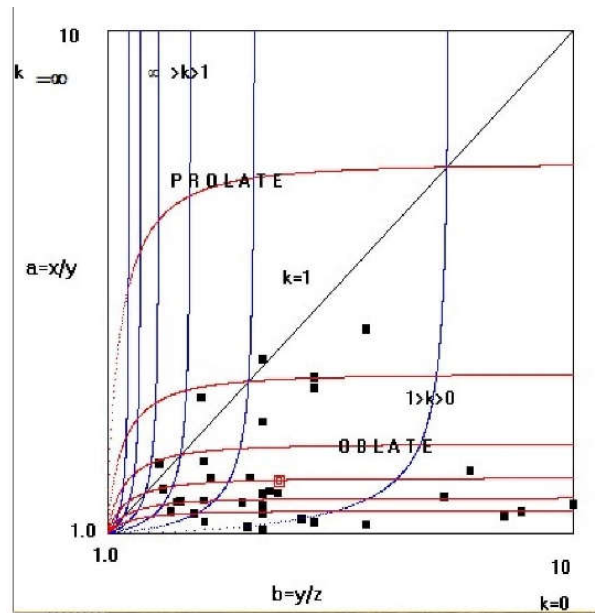


Figure 4e: Flinn diagram for location D5-04

Figure 4(a-e): Flinn plot of Jonk River Conglomerate from D1 to D5 samples

The Flinn plot software is written by *P.P. Roday, 2003*, for Windows 32-Bit Platform Software for plots to display the finite strain data. After obtaining the three-dimensional principal strain values (*Table. 1*), various deformation plots were prepared to depict the deformation. The effect of volume change during the deformation processes was taken into consideration and the results are shown in *table 4*.

Table 1: Result of Flinn Plot for Jonk River Conglomerate

←North		South→		
D1-23 (near Arjuni)	D2-19 (near Rajadevri)	D3-11 (near Sukhri)	D4-07 (near Lukhawpali)	D5-04 (near Matkapali)
a = 1.724 b = 1.89 k = .808 D = .840	a = 2.383 b = 2.517 k = .912 D = 1.267	a = 1.524 b = 1.752 k = .697	a = 2.117 b = 5.109 k = .272	a = 1.93 b = 4.324 k = .248 D = 1.608

4.2 Statistical Mean

In order to determine the 3D geometry of the finite strain ellipsoid in Flinn plot, the above described method was used to estimate the tectonic strain ratios in the XY and YZ principal planes. After the collection of data, the harmonic mean was used as it effectively normalize and give good results (*Lisle, 1977*).

$$\text{The Harmonic Mean (H)} = \frac{n}{\sum(\frac{1}{R_f})} \dots \dots \dots (III)$$

here n= total number of measurements, R_f = final axial ratio of the deformed pebbles. The arithmetic means of these measurements is of little value and will consistently give inaccurate results. Flinn diagram is prepared for each (Fig.4) domain as representative samples with only objective to show deformation plot.

4.3 Elliot polar plot

The simple polar plots that were proposed by *Elliott (1970)* for investigating tectonic deformation. The Elliott polar plot is a polar plot of the natural log R versus 2ϕ . This plot is an equidistant azimuthal hyperboloidal projection (*Yamaji, 2008; Vollmer, 2011; Vollmer, in review*). While all projections have inherent distortion, this plot does not distort strain magnitude radially, and therefore generally provides a better representation of data than the R_f / ϕ plot. In order to evaluate a sample of fabric ellipses prior to further analysis, it is important to plot the data in a way that can identify outliers, modes, and asymmetries. Such a plot is an exploratory evaluation of the density distribution of the data to determine if it can be characterized statistically by a mean and confidence interval, or if it represents a more complex distribution. The R_f / ϕ plot (*Ramsay, 1967; Dunnet, 1969*) and Elliott polar plot are standard plots for ellipse data. It can be shown that these are equidistant hyperboloidal projections, and that other such projections also have useful properties for strain analysis. Figure 5 (a-e) is an Elliott polar plot of the data digitized from the conglomerate photograph. The ellipse means are plotted, and the data has been contoured at 10% of the density distribution. Most of the plots in *EllipseFit* are interactive.

YZ Plane

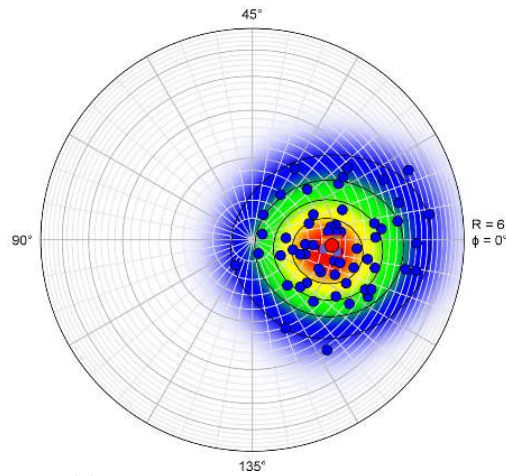


Figure 5(a): D1 - 22, $R = 2.015$
YZ Plane

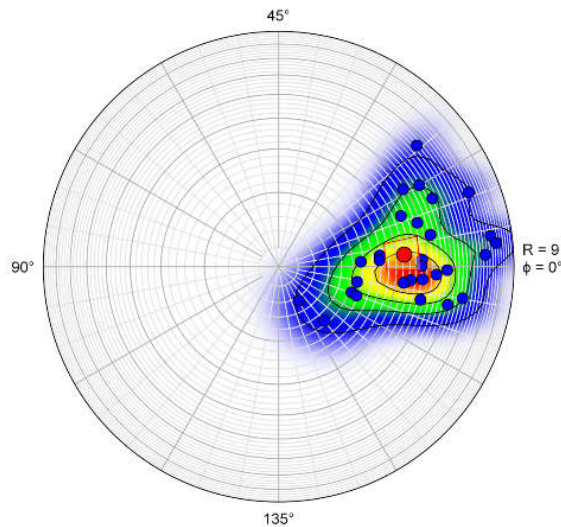


Figure 5(b): D2-17, $R = 3.497$

YZ Plane

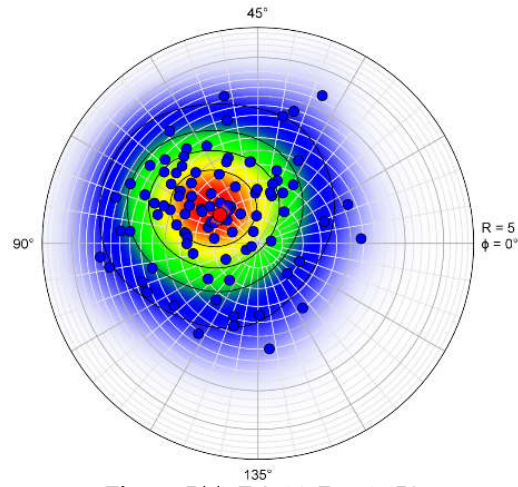


Figure 5(c): D3-14, $R = 1.459$

YZ Plane

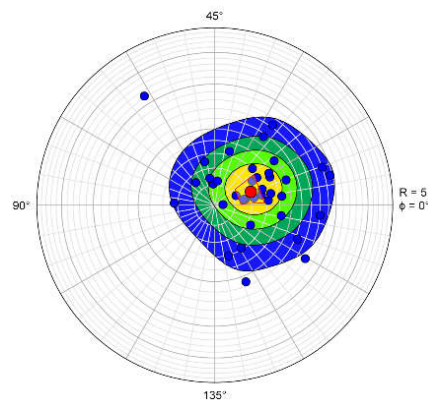


Figure 5(d): D4-08, $R = 1.443$

YZ Plane

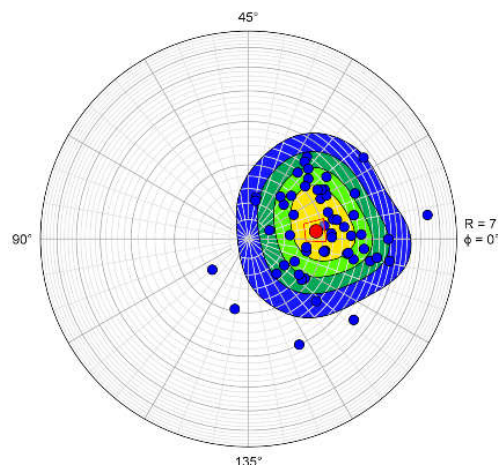


Figure 5(e): D5-02, $R = 1.958$

Figure 5(a-e): Elliott polar plot in the YZ-plane for Jonk River Conglomerate from D1 to D5 samples

Elliott polar plotanalysis data was collected through a standard procedure. We selected a planar surface with pebbles within an area of generally 2m X 2m, of which photograph were collected for further strain analysis with *EllipseFit software*(Vollmer, 2011). Elliott polar plotanalysis of YZ plane uses clast outlines traced from photographs and analysed using *EllipseFit software* developed by Vollmer, 2011. The software automatically approximates shapes to ellipses. Figure 5(a-e) are the different polar diagrams in the YZ-plane for D1 to D5 samples and results are tabulated in table 2.

Result of Elliott polar plot of all five-structural domain from D1(north) to D5(south) is given *Table.2*.

Table 2: Result of Elliott polar plot of YZ plane (Polar Graph Results)

D1-22	D2-17	D3-14	D4-08	D5-02
N = 59 Projection: Logarithmic Centroid: N = 59 R = 2.015 Phi = 177.80° Cumulative percent at or below 5 contour levels:6.8%, 25.4%, 47.5%, 66.1%, 100.0% Cumulative percent at or below 10 contour levels:0.0%, 6.8%, 16.9%, 25.4%, 35.6%, 47.5%, 57.6%, 66.1%, 81.4%, 100.0%	N = 30 Projection: Logarithmic Centroid: N = 30 R = 3.497 Phi = 2.25° Cumulative percent at or below 5 contour levels: 3.3%, 30.0%, 56.7%, 76.7%, 100.0% Cumulative percent at or below 10 contour levels: 0.0%, 3.3%, 13.3%, 30.0%, 43.3%, 56.7%, 66.7%, 76.7%, 83.3%, 100.0%	N = 100 Projection: Logarithmic Centroid: N = 100 R = 1.459 Phi = 71.43° Cumulative percent at or below 5 contour levels:11.0%, 29.0%, 42.0%, 66.0%, 100.0% Cumulative percent at or below 10 contour levels:2.0%, 11.0%, 19.0%, 29.0%, 33.0%, 42.0%, 57.0%, 66.0%, 79.0%, 100.0%	N = 38 Projection: Logarithmic Centroid: N = 38 R = 1.443 Phi = 10.11° Cumulative percent at or below 5 contour levels: 7.9%, 28.9%, 39.5%, 63.2%, 100.0% Cumulative percent at or below 10 contour levels: 2.6%, 7.9%, 23.7%, 28.9%, 36.8%, 39.5%, 52.6%, 63.2%, 71.1%, 100.0%	N = 57 Projection: Logarithmic Centroid: N = 57 R = 1.958 Phi = 3.43° Cumulative percent at or below 5 contour levels:8.8%, 17.5%, 38.6%, 66.7%, 100.0% Cumulative percent at or below 10 contour levels:7.0%, 8.8%, 10.5%, 17.5%, 24.6%, 38.6%, 50.9%, 66.7%, 86.0%, 100.0%

4.4 Fry Method

Fry analysis was done as per earlier described procedure. We use same software (EllipseFit) that we have used for Elliot polar plot. Results from analysis of photographs for five different structural domains (D1 to D5) for same YZ plane as of Elliot polar analysis is given in Table. 3 and shown in Figure 6(a-e).

YZ Plane

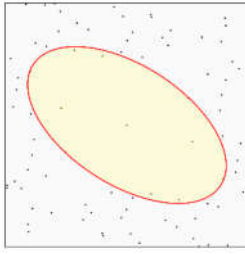


Figure 6(a): D1 - 22, R = 1.870

YZ Plane

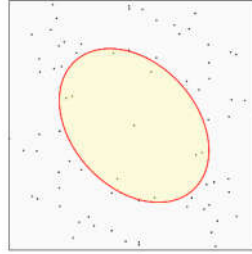


Figure 6(b): D2-17, R = 1.407

YZ Plane

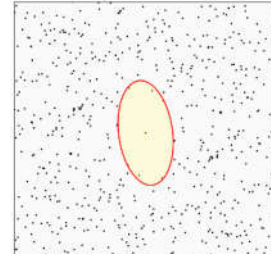


Figure 6(c): D3-14, R = 1.850

YZ Plane

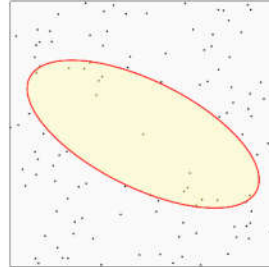


Figure 6(d): D4-08, R = 2.384

YZ Plane

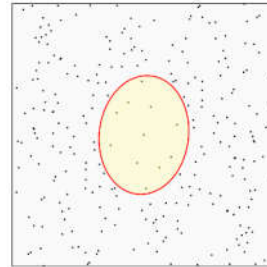


Figure 6(e): D5- 02, R = 1.336

Figure 6(a-e): Fry Plot in the YZ-plane for Jonk River Conglomerate from D1 to D5 samples

The use of one of these methods alone may not furnish an accurate evaluation of finite strain because (i) the harmonic mean is always an overestimate of real strain (*Lisle, 1979*) and (ii) if the Elliot polar plot distribution is not symmetric the method does not provide a correct result. In this study, we used both methods in order to compare results and obtain an estimate of their accuracy. Likewise, the easiest and most used technique for the evaluation of bulk finite strain is the Fry analysis (*Fry, 1979*) is used.

Table 3: Result of Fry analysis of YZ plane

D1	D2	D3	D4	D5
A = 9.152	A = 7.219	A = 0.818	A = 9.547	A = 4.526
B = 4.894	B = 5.129	B = 0.442	B = 4.004	B = 3.387
R = 1.870	R = 1.407	R = 1.850	R = 2.384	R = 1.336
F = 32.54°	F = 48.17°	F = 79.66°	F = 26.47°	F = 96.78°
RMS = 0.0607	RMS = 0.0691	RMS = 0.1266	RMS = 0.0768	RMS = 0.2254

4.5 Logarithmic Flinn Method

The Logarithmic Flinn diagram is a logarithmic version of Flinn diagram introduced by *Ramsay (1967)*, which was also considered and subsequently enlarged by *Ramsay and Wood (1973)*. The main advantage of Ramsay and Woods plot is that we can plot volume change on it. If we consider elongation (e) then,

$$\text{Let, } \ln a = \ln \left(\frac{x}{y} \right) = \ln \left[\frac{1+e_1}{1+e_2} \right]$$

$$\ln b = \ln \left(\frac{y}{z} \right) = \ln \left[\frac{1+e_2}{1+e_3} \right]$$

Using, $\varepsilon = \ln(1 + e)$ and $\ln\left(\frac{x}{y}\right) = \ln x - \ln y$

$$\ln a = \varepsilon_1 - \varepsilon_2$$

$$\ln b = \varepsilon_2 - \varepsilon_3$$

Volume change $\Delta = (V - V_i)/V_i$

$$V = XYZ; V_i = 1$$

$$\Delta = V - 1$$

$$\Delta + 1 = V = XYZ = (1 + e_1)(1 + e_2)(1 + e_3)$$

$$\ln(\Delta + 1) = \varepsilon_1 + \varepsilon_2 + \varepsilon_3$$

This can be rewritten in terms of the Ramsay diagram axes:

$$(\varepsilon_1 - \varepsilon_2) = (\varepsilon_2 - \varepsilon_3) + \ln(\Delta + 1) - 3\varepsilon_2$$

Assume plane strain (i.e. $k=1$; $\square_2 = 0$) on Flinn diagram:

$$(\varepsilon_1 - \varepsilon_2) = (\varepsilon_2 - \varepsilon_3) + \ln(\Delta + 1) \dots \dots \dots (IV)$$

This is the equation no (IV) of straight line at 45° on the Ramsay diagram. Volume loss and flattening plot in same field.

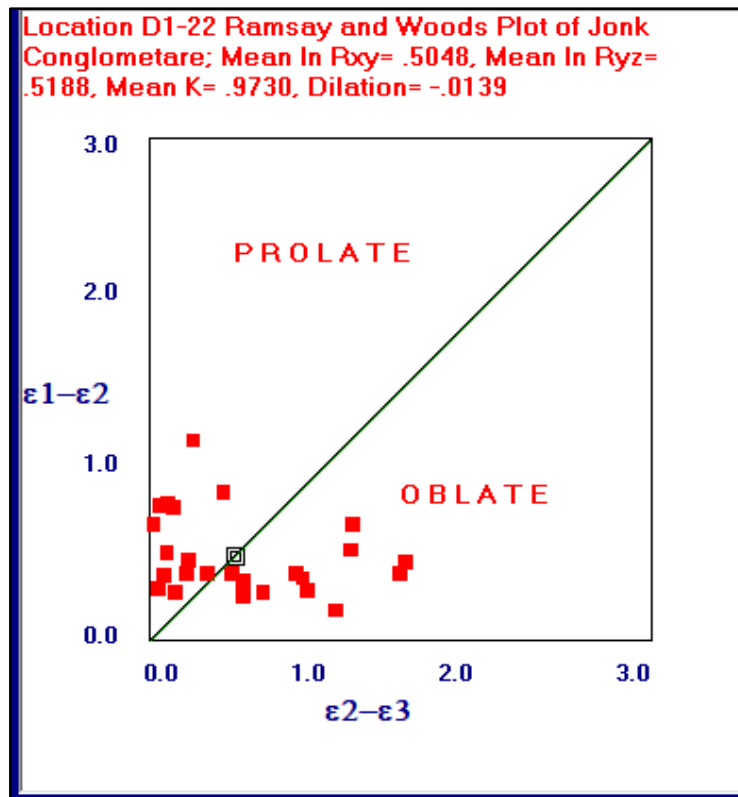


Figure 7(a): Logarithmic Flinn diagram for location D1-23

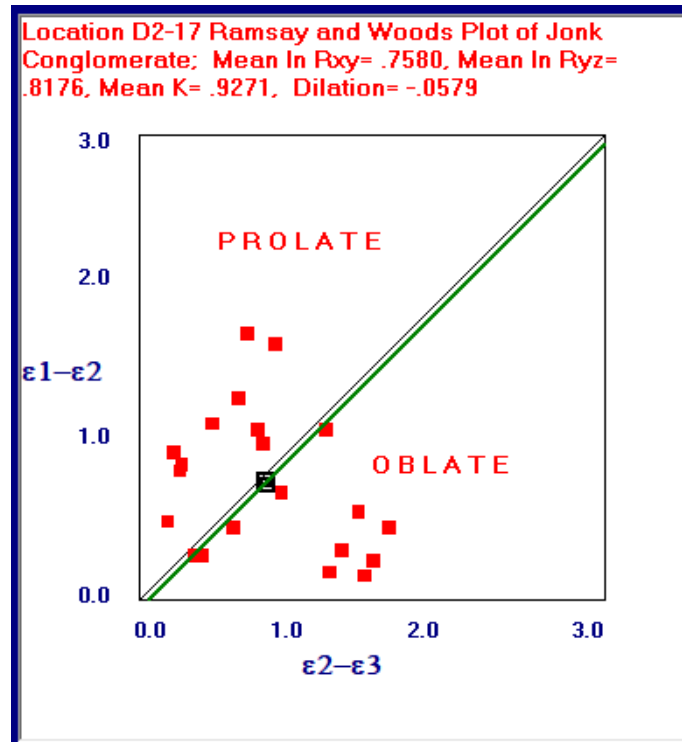


Figure 7(b): Logarithmic Flinn diagram for location D2-19

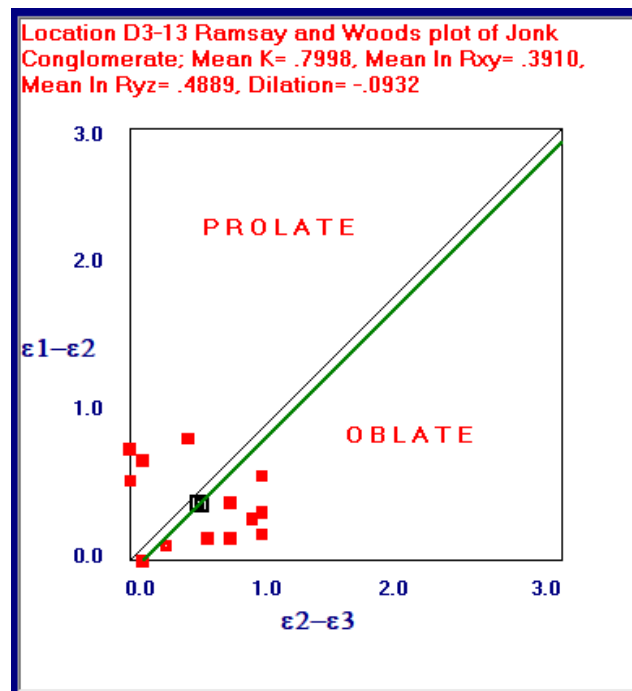


Figure 7(c): Logarithmic Flinn diagram for location D3-11

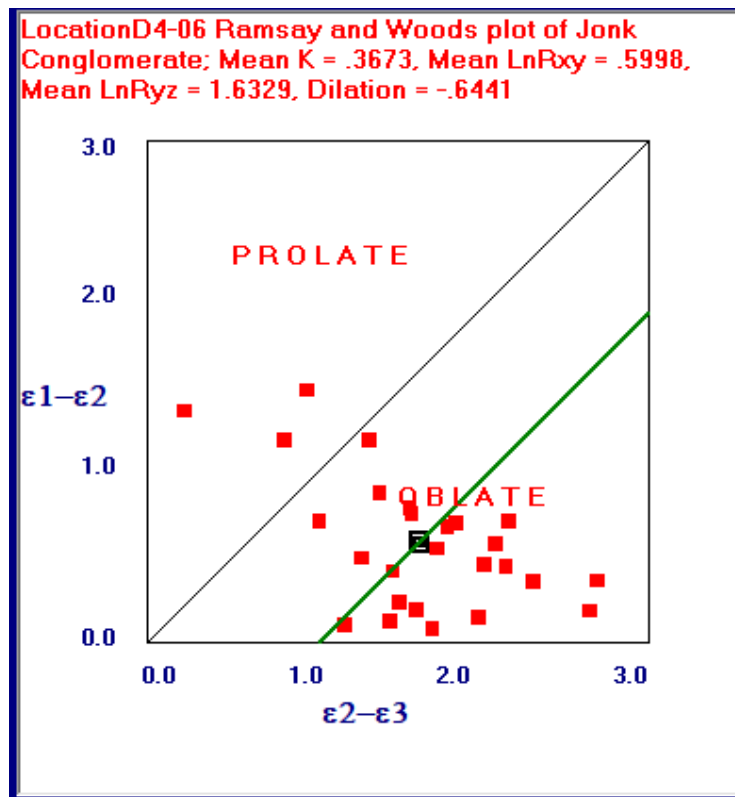


Figure 7(d): Logarithmic Flinn diagram for location D4-07

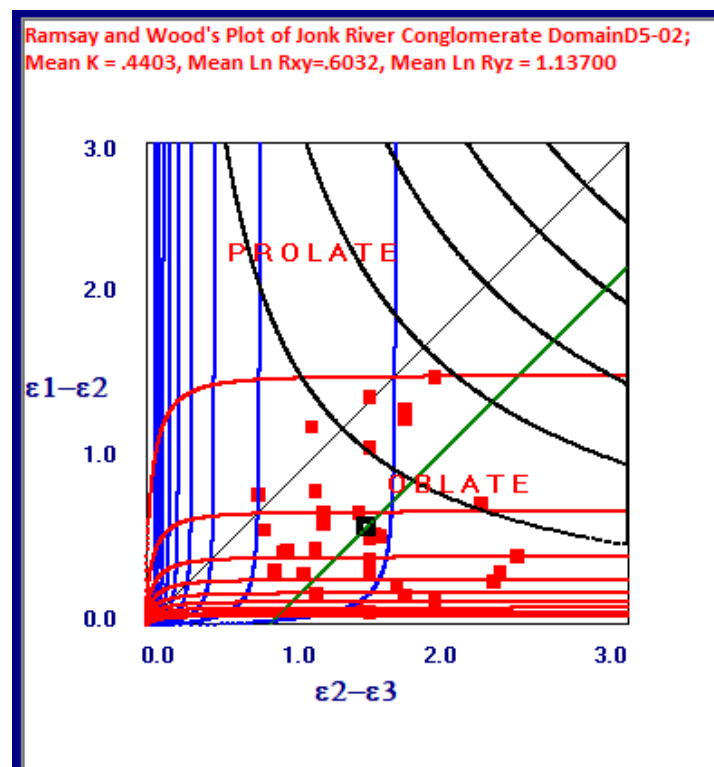


Figure 7(e): Logarithmic Flinn diagram for location D5-04

Figure 7(a-e): Logarithmic Flinn diagrams for Jonk River Conglomerate from D1 to D5 samples

Figure 7(a - e) is Logarithmic Flinn diagram of each arbitrarily chosen structural domain from D1 to D5 of various localities. It is worth to notice that Mean K values progressively approaching lower value from Arjuni (North) to Matkapali (South) and negative dilation data shows consistent volume loss from D1 to D5.

Based on strain result, using software designed by Prakash P. Roday, 2003, the volume loss has been calculated with negative dilation, which means loss of volume.

Table 4: Results of Ramsay & Woods (Logarithmic Flinn) plot of Jonk River Conglomerate

Sample No	Mean Ln Rxy	Mean Ln Ryz	Mean K	Strain Intensity	Dilation
D1-23	0.5048	0.5188	0.973	0.7239	(-).0139
D2-19	0.758	0.8176	0.9271	1.1149	(-).0579
D3-11	0.391	0.4889	0.7998	0.626	(-).0932
D4-07	0.5998	1.6329	0.3673	1.7396	(-).6441
D5-04	0.6032	1.37	0.4403	1.4969	(-).5355

4.6 Volume change and shortening analysis

Strain analysis based on the above results, dilation within D1, D2, D3, D4 and D5 was calculated using Ramsay and Woods plot i.e. logarithmic flinn method uses eqn (IV). The concerned software was developed by Prakash P Roday, 2003. The software provided negative values of dilation which means loss in volume. The strain results of Flinn methods and Logarithmic Flinn methods show consistent volume loss and shortening from D1 to D5. For the D1 strain results shows (-) 1.39% which has lowest volume change out five structural domains. While the greatest volume change is represented by D4 which is (-).5355%. These differences in consistent volume losses from North to South is due to higher content offluid in the D5 (South) may have caused more pressure solution that resulted in more loss of volume of the D5. Second, the D5 is located in the adjacent to the older Baya gneissic complex. For more details about the dilation results see table 5.

Two equations were mentioned by *Onasch (1984)* to calculate the shortening in two different deformation systems.

For the no change in volume deformation shortening can be calculated using:

$$Shortening = \left[1 - \left(\frac{1}{\sqrt{R_{sxz}}} \right) \right] \times 100 \dots \dots \dots (V)$$

For the volume-loss deformation (by pressure solution) the shortening can be calculated by using:

$$Shortening = \left[1 - \left(\frac{1}{R_{sxz}} \right) \right] \times 100 \dots \dots \dots (VI)$$

In this study, the two equations (V) were used to calculate the shortening (Table 5). It is important to mention that using equation (V) means that no assumption of volume change or no pressure solution occurred. On the other hand, using equation (VI) means volume-loss by pressure solution occurred (materials were removed from the rock) (*Onasch, 1984*).

Table 5: Volume Change in Jonk River Conglomerate

Log Flinn Software (Dilation) (%)	Shortening in closed system (Pressure solution, No Volume lost)				
	D1-23 (Ramsay & Woods)	D2-19 (Ramsay & Woods)	D3-11 (Ramsay & Woods)	D4-07 (Ramsay & Woods)	D5-04 (Ramsay & Woods)
	(-)1.39	(-)5.79	(-)9.32	(-)64.41	(-)53.55
Shortening (%) using Onasch,1984 (eqn)	Shortening in open system (Pressure solution, Volume lost)				
	D1-23 HM Rxz (Flinn plot)	D2-19 HM Rxz (Flinn plot)	D3-11 HM Rxz (Flinn plot)	D4-07 HM Rxz (Flinn plot)	D5-04 HM Rxz (Flinn plot)
	38.01838	51.029789	33.62767	65.03582	59.87138
	D1-23 HM Ryz (Flinn plot)	D2-19 HM Ryz (Flinn plot)	D3-11 HM Ryz (Flinn plot)	D4-07 HM Ryz (Flinn plot)	D5-04 HM Ryz (Flinn plot)
	19.93592	30.15697	19.93592	51.83169	47.44117

5. Results and Discussion

Elliot polar plot, Fry Plot, Flinn Polt and logarithmic Flinn plot technique has been used to determine the finite strain ratio in Jonk River Conglomerate horizon, keeping in view the ductility contrast between object and matrix, R_f / ϕ or polar plot (Hyperbolical Projection) may yield an invalid estimation of the strain suffered by the object (DePoar, 1980). Hence, results of two-dimensional strain ratio determined by Polar Plot (Elliot, 1970) and Fry Plot, both shows more or less the same R_s . The polar plot shows R_s of all domain (D1 to D5) range between 3.497 to 1.443, here D2 domain shows exception of $R_s = 3.497$, while D3 to D5 lies within 1.4590 to 1.958. It is worth to notice that North of Jonk River has greater value of $R_s = 2.017$ (D1) while as we move on to South of Jonk River D5 which has tectonic contact with Baya Gneissic shows $R_s = 1.958$, which is least tectonic ratio in whole horizon. Like in same manner the fry method has been carried out, using Ellipsefit Software. The polar plot and fry plot is interchangeable in Ellipsefit. Hence, Fry plot results shows that D1 domain have $R_s = 1.870$ and D5 domain have $R_s = 1.336$, which least tectonic ratio in all domain. Here, D4 domain have exception with $R_s = 2.384$. For the three-dimensional strain analysis, conventional Flinn plot give results as D1 have $k = 0.808$ while D5 having $k = 0.248$, which is least out of all domain. This shows that strain intensity is higher in D5 and lowered down on moving towards north D1. The Flinn Diagram shows that most of deformed objects falls in the oblate to plain strain ellipsoid. Again, Logarithmic Flinn, show the results of various strain parameter. Here, (D1) mean $K = 0.973$ while (D2) mean $K = 0.4403$, which correspond to Flinn Diagram and match with lower value of D5. Hence, we can conclude that differences in the strain data from deformed samples, whereas the behavior between R_f / ϕ and Fry methods are the same order of the deformation. The strain intensity, as obtained from Logarithmic Flinn, have average ranging from 0.7239 to 1.7396, which indicate a very heterogeneous deformation (Table 4). The dilation results, as obtained from Logarithmic Flinn, ranged from (-)1.39 to (-)64.41, negative dilation data shows consistent volume loss from D1 to D5. The difference in the dilation may be of two reasons, first, tectonic contact between Baya Gneiss and conglomerate (D5) has compacted more time and have greater volume loss (Table 5). Second, more compaction means more fluid content probably occurred in D5 domain during deformation. This higher content of fluid in the D5 may have caused more pressure solution that resulted in more loss of volume.

6. Conclusion

Our data show that the Jonk River Conglomerate are characterized by the shortening axes are subvertical associated with a sub horizontal foliation in the area (Table 5). We can also conclude the heterogeneous deformation at all domains. The Ramsay & Woods diagram (Figure 7) shows that most of the object finite strain ellipsoids inferred from the deformed pebbles fall into the oblate field,

although they plot close to the plane strain line. In addition, we can also conclude, the volume loss at all domain, from D1 to D5.

Acknowledgement

The present work is a part PhD of KC. Author is very much thankful to all faculty of NITRR and Hon'ble Director of NITRR for arranging field work programme every year while author staying at NITRR. Our thanks to F. W Vollmer for his software EllipseFit and Late Prof. P.P. Roday for his software Flinn Plot and Ramsay and Woods plot software from which most strain analysis has been done. Author is also thankful to the anonymous reviewer for critically reviewing the manuscript and offering constructive comments.

Reference

1. Babaie, H. A., 1986, A comparison of Two-Dimensional Strain Methods Using Elliptical Grains: *Journal of Structural Geology*, vol. 8, No. 5, pp. 585-587.
2. Burns, K. L., Spry, A. H., 1969. Analysis of shape of deformed pebbles; *Tectonophys.* 7 177-196.
3. Chawade, M.P., 2010, Sonakhan Granite Greenstone Belt, unpublished report, Central Region, Geological Survey of India.
4. Das, N., Royburman, K. J., Vasta, U. S., and Mahurkar, Y.V, 1990. Sonakhan schist belt - a Precambrian granite-greenstone complex. GSI Spl. Pub. No. 28, 118-132.
5. DePaor, D. G., 1980, Some limitation of R_f/ϕ techniques of strain analysis. *Tectonophysics*, Vol. 64, T29 – T31.
6. Dunnet, D., 1969. A technique of finite strain analysis using elliptical particles. *Tectonophysics* 7, 117-136.
7. Elliott, D., 1970, Determination of finite strain and initial shape from deformed elliptical objects: *Geol. Soc. Am. Bull.*, v. 81, p. 2221-2236.
8. Flinn, D., 1962. On folding during three-dimensional progressive deformation. *Quarterly Journal of Geological Society*, London 118, 385-433.
9. Fry, N., 1979 Random point distributions and strain measurement in rocks; *Tectonophysics*. 60 89-105.
10. Gay, N.C., 1969. Analysis of strain in the Barberton Mountain Land, eastern Transvaal, using deformed pebbles. *Journal of Geology* 77, pp377-396.
11. Hossack, J. R., 1968 Pebble deformation and thrusting in the Bygdin area; *Tectonophys.* 5 315-319.
12. Lisle, R.J., 1977. Estimation of the tectonic strain ratio from the mean shape of deformed elliptical markers. *Geologie en Mijnbouw* 56, 140-144.
13. Lisle, R.J., 1979. Strain analysis using deformed pebbles: the influence of initial pebble shape. *Tectonophysics* 60, 263 - 277
14. Mondal, M., Raza, M. 2009. Tectonomagmatic evolution of the Bastar craton of Indian shield through plume-arc interaction: evidence from geochemistry of the mafic and felsic volcanic rocks of Sonakhan greenstone belt. In: (Eds.) Talat Ahmad, Francis Hirsch, and Punya Charusiri, *Journal of the Virtual Explorer*, volume 32, paper 7, doi: 10.3809/jvirtex.2009.00245
15. Mulchrone, K. F., Meere, P. A., and Choudhury, K. R., 2005, SAPE: a program for semi-automatic parameter extraction for strain analysis: *Journal of Structural Geology*, vol. 27, pp. 2084-2098.
16. Onasch, C. M., 1984, Application of the R_f/ϕ technique to elliptical markers deformed by pressure-solution: *Tectonophysics*, v. 110, p. 157-165.
17. Ramsay, J.G., 1967. *Folding and Fracturing of Rocks*. McGraw Hill, New York.
18. Ramsay, J.G., Huber, M.I., 1983. *The Techniques of Modern Structural Geology*, vol. 1. Strain Analysis, Academic Press, London.
19. Ramsay, J.G., Wood, D.S., 1973. The geometric effects of volume change during deformation processes. *Tectonophysics* 16, 263-277.

20. Roday, P. P., 2003 Windows 32-Bit Platform Software for Plots to Display the Finite Strain Data Journal Geological Society of India Vol.62, July 2003, Pp.36-42
21. Roday, P.P., Katpatal Y.B., (1993), "Departures from true ellipticity of principle sectional boudin shapes and their mechanical and kinematic implecations", Journ. Geol. Soc. Ind., Vol.42, Issue 1. July 1993, PP 39-49.
22. Treagus, S. H., and Treagus, J. E., 2002, Studies of Strain and Rheology of Conglomerates: Journal of Structural Geology, vol. 24, pp. 1541-1567.
23. Vollmer, F. W., 2011. Automatic contouring of two-dimensional finite strain data on the unit hyperboloid and the use of hyperboloidal stereographic, equal-area and other projections for strain analysis. Geological Society of America Abstracts with Programs, v. 43, n. 5, p. 605.
24. Vollmer, F. W., 2011. Best-fit strain from multiple angles of shear and implementation in a computer program for geological strain analysis. Geological Society of America Abstracts with Programs, v. 43.
25. Yamaji, A., 2008. Theories of strain analysis from shape fabrics: A perspective using hyperbolic geometry. Journal of Structural Geology 30, 1451-1465.